

Controlling higher-order quantum nonreciprocity by spinning an optical resonator

Yonglin Xiang,^{1,*} Yunlan Zuo,^{1,*} Xun-Wei Xu,¹ Ran Huang,² and Hui Jing^{1,3,†}

¹*Key Laboratory of Low-Dimensional Quantum Structures and Quantum Control of Ministry of Education, Department of Physics and Synergetic Innovation Center for Quantum Effects and Applications, Hunan Normal University, Changsha 410081, China*

²*Theoretical Quantum Physics Laboratory, RIKEN Cluster for Pioneering Research, Wako-shi, Saitama 351-0198, Japan*

³*Synergetic Innovation Academy for Quantum Science and Technology, Zhengzhou University of Light Industry, Zhengzhou 450002, China*

(Dated: April 3, 2023)

We study how to achieve, manipulate, and switch classical or quantum nonreciprocal effects of light with a spinning Kerr resonator. In particular, we show that even when there is no classical nonreciprocity (i.e., with the same mean number of photons for both clockwise and counterclockwise propagating modes), it is still possible to realize nonreciprocity of quantum correlations of photons in such a device. Also, by tuning the angular velocity and the optical backscattering strength, higher-order quantum nonreciprocity can appear, featuring qualitatively different third-order optical correlations, even in the absence of any nonreciprocity for both the mean photon number and its second-order correlations. The possibility to switch a single device between a classical isolator and a purely quantum directional system can provide more functions for nonreciprocal materials and new opportunities to realize novel quantum effects and applications, such as nonreciprocal multi-photon blockade, one-way photon bundles, and backaction-immune quantum communications.

I. INTRODUCTION

Optical nonreciprocity, featuring different responses of light when the input and output ports are interchanged, plays a key role in fundamental studies and applications of modern optics, such as directional laser engineering, invisible sensing, and backaction-immune optical communications [1]. In recent years, without using any bulky magnetic material [2, 3], various ways have been demonstrated to create optical on-chip nonreciprocity, such as spatiotemporal modulation [4–11], optical nonlinearities [12–31], non-Hermitian structures [32–35], quantum squeezing [36], and controllable motion of atoms or solid devices [37–61]. Particularly, by spinning a single device, it is possible to achieve nonreciprocal transmissions of light, sound, or thermal filed, without relying on any nonlinear medium [62–64], providing flexible new ways to achieve nanoparticle sensing [65–67], optical gyroscopes [68], and quantum or topological directional control [69–73]. Also, by further integrating with existing techniques of quantum nonlinear optics, purely quantum nonreciprocal effects can be achieved in such spinning systems, such as nonreciprocal photon blockade [46–50] and nonreciprocal quantum entanglement [51–54]. We note that, in a very recent experiment, quantum nonreciprocal correlations of photons were already observed in experiments using cavity atoms or an optical nonlinear system [74, 75]. However, till now, in the absence of any classical nonreciprocity, the possibility of achieving one-way control of higher-order quantum correlations, has not yet been studied.

Here, in this work, we show how to achieve coherent switch of classical and quantum nonreciprocities of photons, and how to realize higher-order quantum nonreciprocity with a single spinning resonator. We find that, by tuning both the angular speed of the resonator and the optical backscattering strength, one can switch the functions of the device between a classical isolator and a purely quantum directional system. Also, a new class of higher-order quantum nonreciprocity, i.e., when both the mean photon numbers and the second-order correlations are reciprocal, the third-order correlation function is nonreciprocal. Particularly, we note that the backscattering due to material imperfections can induce a higher-order quantum nonreciprocal effect, in comparison with that in ideal devices. Our findings indicate a promising new way to achieve novel nonreciprocal effects, which is useful in realizing chiral quantum networks [76–79] and invisible sensing [80, 81].

The remainder of this paper is organized as follows. In Sec. II, we introduce the physical system of a spinning Kerr resonator with a tapered fiber. In Sec. III, we study the quantum and classical nonreciprocities in the ideal spinning resonator. In Sec. IV, we explore the quantum and classical nonreciprocities for systems with backscattering. In particular, revealing a novel higher-order quantum nonreciprocity. In Sec. V, we give a summary.

II. PHYSICAL SYSTEM

As shown in Fig. 1(a), we consider a spinning Kerr resonator evanescently coupled with a tapered fiber, and each side of the fiber serves as both an input port and an output port. Depending on the input port, light is coupled to circulate in the resonator in either

* These authors contributed equally to this work.

† jinghui73@foxmail.com

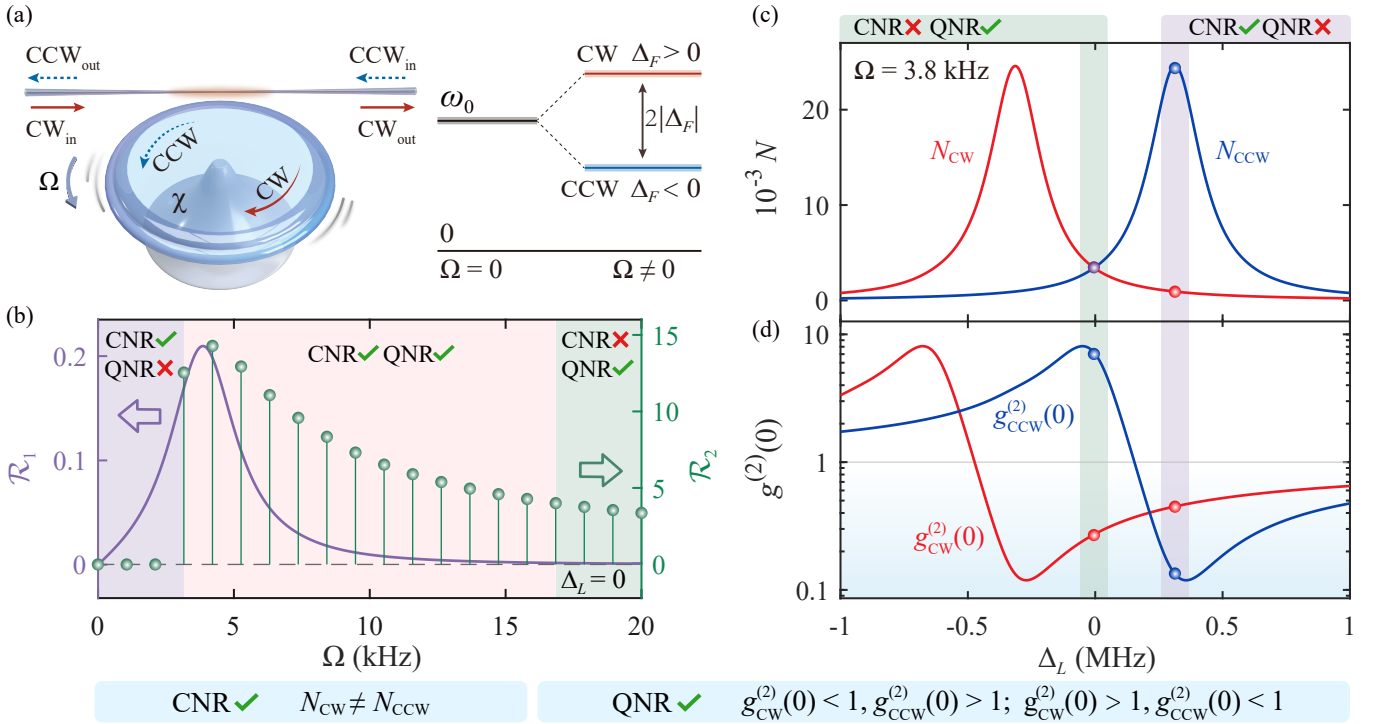


FIG. 1. Quantum and classical nonreciprocities. (a) The whispering-gallery-mode resonator with Kerr-type nonlinearity χ spinning at an angular velocity Ω . By fixing the CCW rotation of the resonator, the $\Delta_F > 0$ ($\Delta_F < 0$) corresponds to the situation of driving the CW (CCW) mode. (b) The classical (quantum) nonreciprocity ratio \mathcal{R}_1 (\mathcal{R}_2) versus the angular velocity Ω for $\Delta_L = 0$. (c) The mean photon number N and (d) the second-order correlation function $g^{(2)}(0)$ versus the optical detuning Δ_L for different input directions at $\Omega = 3.8$ kHz. The parameters are given in the main text.

the clockwise (CW) or the counterclockwise (CCW) direction. Recently, 99.6% optical isolation was realized experimentally by using a spinning resonator [44]. In this experiment, the resonator is mounted on a turbine and rotated along its axis. The tapered fiber is made by heating and pulling a standard single-mode telecommunications fiber, which is stabilized at the height of several nanometers above the rapidly spinning resonator via the “self-adjustment” aerodynamic process. Here, for a resonator spinning along a fixed direction at an angular velocity Ω , the resonance frequencies of the CW and CCW modes experience an opposite Sagnac-Fizeau shift, i.e., $\omega_0 \rightarrow \omega_0 + \Delta_F$, with [82]

$$\Delta_F = \pm \frac{n_1 r \Omega \omega_0}{c} \left(1 - \frac{1}{n_1^2} - \frac{\lambda}{n_1} \frac{dn_1}{d\lambda} \right), \quad (1)$$

where ω_0 is the optical frequency of the nonspinning resonator, $c(\lambda)$ is the speed (wavelength) of light in a vacuum, n_1 and r are the refractive index and radius of the resonator, respectively. The dispersion term $dn_1/d\lambda$, characterizing the relativistic origin of the Sagnac effect, is relatively small in typical materials (up to about 1%) [44, 82]. By spinning the resonator along the CCW direction, we have $\Delta_F > 0$ ($\Delta_F < 0$) for the case with the driven the CW (CCW) mode, i.e., $\omega_{\text{cw,ccw}} = \omega_0 \pm |\Delta_F|$, see Fig. 1(a).

In the frame rotating at the drive frequency ω_L , the Hamiltonian of the system reads ($\hbar = 1$)

$$\hat{H}_1 = (\Delta_L + \Delta_F) \hat{a}^\dagger \hat{a} + \chi \hat{a}^\dagger \hat{a}^\dagger \hat{a} \hat{a} + \xi (\hat{a}^\dagger + \hat{a}), \quad (2)$$

where $\Delta_L = \omega_0 - \omega_L$ is the optical detuning between the driving field and the cavity field, \hat{a} (\hat{a}^\dagger) is the optical annihilation (creation) operator, $\chi = \hbar \omega_0^2 c n_1 / (n_0^2 V_{\text{eff}})$ is the Kerr parameter, with the linear (nonlinear) refraction index n_0 (n_2), and the effective mode volume V_{eff} . The $\xi = \sqrt{\gamma P_{\text{in}} / (\hbar \omega_L)}$ is driving amplitude with the cavity loss rate γ and the driving power P_{in} .

The energy eigenstates of this system are the Fock states $|n\rangle$ ($n = 0, 1, 2, \dots$) with eigenenergies

$$E_n = n \Delta_L + n \Delta_F + (n^2 - n) \chi, \quad (3)$$

where n is the cavity photon number. The positive and negative values of Δ_F describing upper or lower shifts of energy levels, respectively [Fig. 1(a)], and the values of $|\Delta_F|$ with an amount being proportional to Ω . For the same input light, due to the opposite frequency shift for the counterpropagating modes, nonreciprocity can appear.

The experimentally accessible parameters we used here are [83–87]: $\lambda = 1550$ nm, $Q = 5 \times 10^9$, $V_{\text{eff}} = 150 \mu\text{m}^3$, $n_2 = 2 \times 10^{-15} \text{ m}^2/\text{W}$ [83], $n_0 = 1.4$, $P_{\text{in}} = 0.2$ fW, and $r = 30 \mu\text{m}$. V_{eff} is typically 10^2 – $10^4 \mu\text{m}^3$ [84, 85], Q is typically 10^9 – 10^{12} [86, 87].

III. QUANTUM AND CLASSICAL NONRECIPROCITIES

The quantum features of this work can be characterized by the quantum correlation function $g^{(2)}(0)$:

$$g^{(2)}(0) = \frac{\langle \hat{a}^\dagger \hat{a}^2 \rangle}{\langle \hat{a}^\dagger \hat{a} \rangle^2}, \quad (4)$$

where $N = \langle \hat{a}^\dagger \hat{a} \rangle$ is the classical mean photon number. The conditions $g^{(2)}(0) < 1$ characterize photon blockade, but not vice versa. Thus, the condition of quantum nonreciprocity (QNR) is given by

$$g_{\text{CW}}^{(2)}(0) < 1, \quad g_{\text{CCW}}^{(2)}(0) > 1,$$

or

$$g_{\text{CW}}^{(2)}(0) > 1, \quad g_{\text{CCW}}^{(2)}(0) < 1. \quad (5)$$

The condition of classical nonreciprocity (CNR) is

$$N_{\text{CW}} \neq N_{\text{CCW}}. \quad (6)$$

For this work, we use subscripts CW and CCW to denote the cases with the driven the CW and CCW modes, respectively.

To better study the classical and quantum nonreciprocities of this system, we define the classical and quantum nonreciprocity ratios as \mathcal{R}_1 and \mathcal{R}_2 , respectively, which are written as

$$\begin{aligned} \mathcal{R}_1 &= 10 \log_{10} \frac{N_{\text{CCW}}}{N_{\text{CW}}}, \\ \mathcal{R}_2 &= 10 \log_{10} \frac{g_{\text{CCW}}^{(2)}(0)}{g_{\text{CW}}^{(2)}(0)}. \end{aligned} \quad (7)$$

When N_{CW} and N_{CCW} do not satisfy the condition of nonreciprocity in Eq. (6), i.e., classical reciprocity, $\mathcal{R}_1 = 0$. Similarly, when $g_{\text{CW}}^{(2)}(0)$ and $g_{\text{CCW}}^{(2)}(0)$ do not satisfy the condition of nonreciprocity in Eq. (5), i.e., quantum reciprocity, we set $\mathcal{R}_2 = 0$.

According to the quantum-trajectory method [88], the optical decay can be included in the effective Hamiltonian

$$\hat{H}_{\text{e1}} = \hat{H}_1 - i \frac{\gamma}{2} \hat{a}^\dagger \hat{a}, \quad (8)$$

with $\gamma = \omega_0/Q$ is the cavity loss rate with the quality factor Q . Under the weak-driving condition ($\xi \ll \gamma$), the Hilbert space can be truncated to $n = 2$. The state of this system can be expressed as

$$|\varphi(t)\rangle = \sum_{n=0}^2 C_n(t) |n\rangle, \quad (9)$$

with probability amplitudes C_n . Based on the effective Hamiltonian in Eq. (8), and the wave function in Eq. (9),

we can obtain the following equations of motion for the probability amplitudes $C_n(t)$:

$$\begin{aligned} \dot{C}_0(t) &= -iE_0 C_0(t) - i\xi C_1(t), \\ \dot{C}_1(t) &= -i \left(E_1 - i \frac{\gamma}{2} \right) C_1(t) - i\xi C_0(t) - i\xi \sqrt{2} C_2(t), \\ \dot{C}_2(t) &= -i(E_2 - i\gamma) C_2(t) - i\xi \sqrt{2} C_1(t), \end{aligned} \quad (10)$$

where $E_0 = 0$, $E_1 = \Delta_L + \Delta_F$, $E_2 = 2(\Delta_L + \Delta_F) + 2\chi$. In the weak-driving case, these probability amplitudes have the following approximation expressions: $C_0 \sim 1$, $C_1 \sim \xi/\gamma$, and $C_2 \sim \xi^2/\gamma^2$. According to perturbation method [89] to solve the above equations, we can obtain the probability amplitudes as

$$\begin{aligned} \dot{C}_0(t) &= -iE_0 C_0(t), \\ \dot{C}_1(t) &= -i \left(E_1 - i \frac{\gamma}{2} \right) C_1(t) - i\xi C_0(t), \\ \dot{C}_2(t) &= -i(E_2 - i\gamma) C_2(t) - i\xi \sqrt{2} C_1(t). \end{aligned} \quad (11)$$

In an initially empty cavity, the initial conditions can be set as:

$$\begin{aligned} C_0(0) &= C_0(0), \\ C_1(0) &= C_2(0) = 0. \end{aligned} \quad (12)$$

Therefore, we can obtain the solution of the zero-photon amplitude:

$$C_0(t) = C_0(0) \exp(-iE_0 t). \quad (13)$$

We introduce the slow-varying amplitudes to solve this equation:

$$\begin{aligned} C_1(t) &= c_1(t) \exp \left[-i(E_1 - i \frac{\gamma}{2}) t \right], \quad C_1(0) = c_1(0), \\ C_2(t) &= c_2(t) \exp \left[-i(E_2 - i\gamma) t \right], \quad C_2(0) = c_2(0). \end{aligned} \quad (14)$$

Then, based on the solution of the zero-photon amplitude in Eq. (13) and the above equations, we can obtain the solutions of the equations of motion for the probability amplitudes

$$\begin{aligned} C_0(t) &= C_0(0) \mathcal{A}_0, \\ C_1(t) &= -\xi C_0(0) (\mathcal{A}_0 - \mathcal{A}_1) / \left(E_1 - i \frac{\gamma}{2} \right), \\ C_2(t) &= \sqrt{2} \xi^2 C_0(0) (\mathcal{B}_0 - \mathcal{B}_1) / \left(E_1 - i \frac{\gamma}{2} \right), \end{aligned} \quad (15)$$

where

$$\begin{aligned} \mathcal{A}_0 &= \exp(-iE_0 t), \\ \mathcal{A}_1 &= \exp[-i(E_1 - i\gamma/2) t], \\ \mathcal{A}_2 &= \exp[-i(E_2 - i\gamma) t], \\ \mathcal{B}_0 &= (\mathcal{A}_0 - \mathcal{A}_2) / (E_2 - E_0 - i\gamma), \\ \mathcal{B}_1 &= (\mathcal{A}_1 - \mathcal{A}_2) / (E_2 - E_1 - i\gamma/2), \end{aligned} \quad (16)$$

and for the infinite-time limit, we have $\exp(-At) \rightarrow 0$ ($t \rightarrow \infty$), then the solutions should be

$$\begin{aligned} C_0 &\equiv C_0(\infty) = 1, \\ C_1 &\equiv C_1(\infty) = \frac{-\xi}{(E_1 - i\gamma/2)}, \\ C_2 &\equiv C_2(\infty) = \frac{-\sqrt{2}\xi C_1}{(E_2 - i\gamma)}. \end{aligned} \quad (17)$$

According to the normalized coefficient of the state

$$\mathcal{M} = 1 + |C_1|^2 + |C_2|^2, \quad (18)$$

we can get the probabilities of finding n photons in the resonator as

$$P_n = \frac{|C_n|^2}{\mathcal{M}}. \quad (19)$$

The mean photon number is denoted by N , and can be obtained from the above probability distribution as

$$N = \langle \hat{a}^\dagger \hat{a} \rangle \simeq \frac{\xi^2}{(\Delta_L + \Delta_F)^2 + \gamma^2/4}. \quad (20)$$

The equal-time (namely zero-time-delay) second-order correlation function is written as

$$g^{(2)}(0) = \frac{\langle \hat{a}^\dagger \hat{a}^2 \rangle}{\langle \hat{a}^\dagger \hat{a} \rangle^2} \simeq \frac{(\Delta_L + \Delta_F)^2 + \gamma^2/4}{(\Delta_L + \Delta_F + \chi)^2 + \gamma^2/4}. \quad (21)$$

To obtain more exact results, we numerically study the full quantum dynamics of the system by solving the master equation [90, 91]

$$\dot{\hat{\rho}} = \frac{i}{\hbar} [\hat{\rho}, \hat{H}_1] + \frac{\gamma}{2} (2\hat{a}\hat{\rho}\hat{a}^\dagger - \hat{a}^\dagger\hat{a}\hat{\rho} - \hat{\rho}\hat{a}^\dagger\hat{a}), \quad (22)$$

where $\hat{\rho}$ is the normalized density matrix of the system. The photon-number probability is $P_n = \langle n | \hat{\rho}_{ss} | n \rangle$, with the steady-state solutions $\hat{\rho}_{ss}$ of the master equation.

Figure 1(b) shows the switching between CNR and QNR when the optical detuning $\Delta_L = 0$. For a non-spinning resonator ($\Omega = 0$), both classical and quantum effects are reciprocal at this point, i.e., $\mathcal{R}_1 = 0$ and $\mathcal{R}_2 = 0$. When the angular velocity Ω below 3 kHz, the classical nonreciprocity ratio $\mathcal{R}_1 \neq 0$, i.e., classical nonreciprocity. At the same time, the quantum nonreciprocity ratio \mathcal{R}_2 is always equal to 0, the quantum effect is reciprocal. On the contrary, when the Ω exceeds 17 kHz, $\mathcal{R}_1 = 0$ and $\mathcal{R}_2 \neq 0$, this means that quantum nonreciprocity exists even when there is no classical nonreciprocity. Thus, we find different nonreciprocities that can be tuned by adding the angular velocity.

In addition, we note that the switching between classical nonreciprocity and pure quantum nonreciprocity can also be achieved by tuning the optical detuning Δ_L [Figs. 1(c) and 1(d)]. As an illustration, for a spinning cavity, by driving the CW (CCW) mode, we have $\Delta_F > 0$ ($\Delta_F < 0$), thus, leading to quantum nonreciprocity at

$\Delta_L = 0$, i.e., $g_{\text{CW}}^{(2)}(0) \sim 0.28$, $g_{\text{CCW}}^{(2)}(0) \sim 7$. At this point, $N_{\text{cw}} = N_{\text{ccw}}$, the classical effect is reciprocal. When the maximum difference of mean photon numbers by driving the setup from the right and left sides is generated, i.e., $N_{\text{CW}} \sim 0.001$ and $N_{\text{CCW}} \sim 0.0245$. This is a clear signature of classical nonreciprocity. At the same time, we have quantum reciprocity, i.e., $g_{\text{CW}}^{(2)}(0) \sim 0.45$ and $g_{\text{CCW}}^{(2)}(0) \sim 0.12$.

These results show that a single device switching between a classical isolator and a quantum one-way device can be achieved by adjusting multiple degrees of freedom [51].

IV. QUANTUM AND CLASSICAL NONRECIPROCITIES WITH BACKSCATTERING

Now, we further extend our present study to a more generalized situation. In practice, the imperfections of devices, such as surface roughness or material defect, can cause optical backscattering, as shown in Fig. 2(a). Thus, we discuss the role of backscattering in quantum and classical nonreciprocities. For this aim, we introduce backscattering, as described by the coupling strength J between the CW and CCW modes. The system's Hamiltonian, given in Eq. (2), is transformed to

$$\begin{aligned} \hat{H}_2 = & \sum_{j=1,2} \Delta_j \hat{a}_j^\dagger \hat{a}_j + \sum_{j=1,2} \chi \hat{a}_j^\dagger \hat{a}_j^\dagger \hat{a}_j \hat{a}_j \\ & + 2\chi \hat{a}_1^\dagger \hat{a}_1 \hat{a}_2^\dagger \hat{a}_2 + J (\hat{a}_1^\dagger \hat{a}_2 + \hat{a}_2^\dagger \hat{a}_1) \\ & + \xi (\hat{a}_1^\dagger + \hat{a}_1), \end{aligned} \quad (23)$$

where $\hat{a}_1(\hat{a}_1^\dagger)$ and $\hat{a}_2(\hat{a}_2^\dagger)$ are the annihilation (creation) operators of the CW and CCW modes, respectively. And $\Delta_j = \Delta_L \pm |\Delta_F| (j = 1, 2)$, $2\chi \hat{a}_1^\dagger \hat{a}_1 \hat{a}_2^\dagger \hat{a}_2$ is the cross-Kerr interaction [14, 92] between the CW and CCW modes.

Optical decay can be included in the effective Hamiltonian [88],

$$\hat{H}_{e2} = \hat{H}_2 - \sum_{j=1,2} i\gamma \hat{a}_j^\dagger \hat{a}_j / 2. \quad (24)$$

In the weak-driving case ($\xi \ll \gamma$), the Hilbert space of the system can be restricted to a subspace with few photons. Here, in order to calculate the expressions of the second-order and third-order correlation functions, this Hilbert space is truncated to a subspace with three-photon numbers, i.e., $N = m + n = 3$, the wave function of the system can be expressed as

$$|\psi(t)\rangle = \sum_{N=0}^3 \sum_{m=0}^N C_{m,N-m} |m, N-m\rangle, \quad (25)$$

where C_{mn} are probability amplitudes corresponding to state $|m, n\rangle$. By solving the Schrödinger equation

$$i|\dot{\psi}(t)\rangle = \hat{H}_{e2} |\psi(t)\rangle, \quad (26)$$

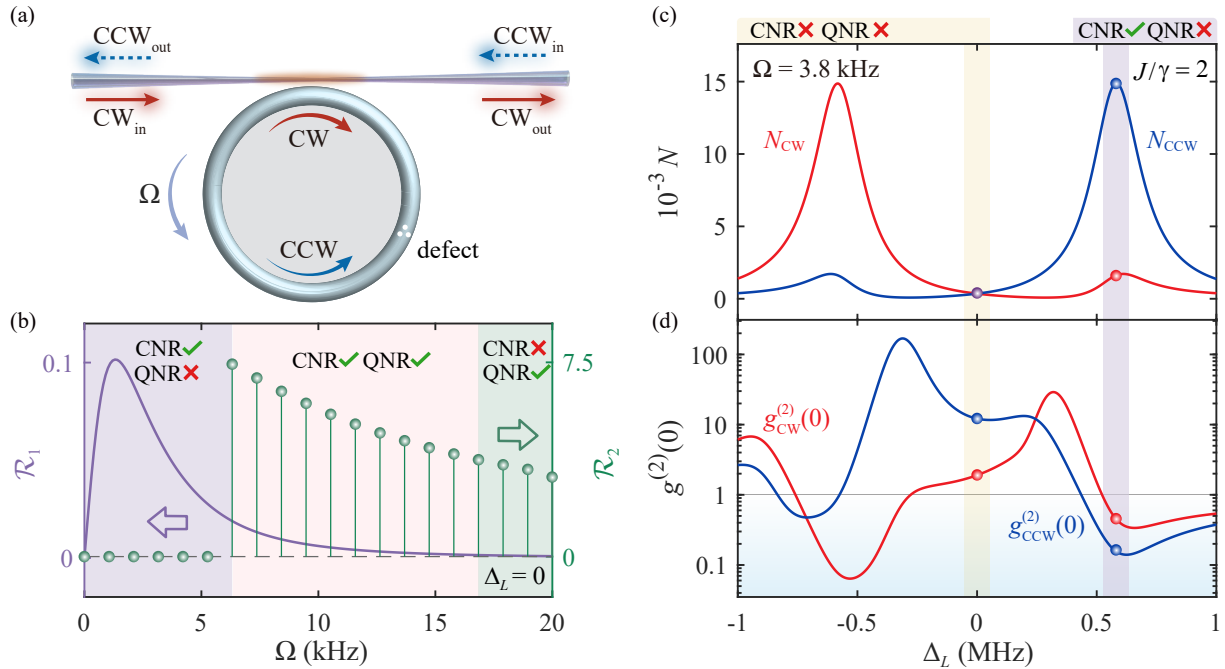


FIG. 2. Quantum and classical nonreciprocities with backscattering. (a) The spinning Kerr resonator with defect-induced backscattering. The CW and CCW modes are coupled via backscattering with the strength J . (b) The classical (quantum) nonreciprocity ratio \mathcal{R}_1 (\mathcal{R}_2) versus the angular velocity Ω for $\Delta_L = 0$. (c) The mean photon number N and (d) the second-order correlation function $g^{(2)}(0)$ as functions of Δ_L for different input directions at $\Omega = 3.8$ kHz. The parameter of mode-coupling strength is chosen as $J/\gamma = 2$, the other parameters are the same as those in Fig. 1.

we can obtain the above probability amplitudes C_{mn} . When a weak-driving field is applied to the cavity, it may excite few photons in the cavity. Therefore, we can approximate the probability amplitudes of the excitations as $C_{m,N-m} \sim (\xi/\gamma)^N$. Here, we use the perturbation method [89] to solve the equations of motion for the probability amplitudes $C_{m,N-m}(t)$. Then, we have the equations of motion for probability amplitudes

$$\begin{aligned}
i\dot{C}_{00}(t) &= 0, \\
i\dot{C}_{01}(t) &= \Delta_4 C_{01}(t) + J C_{10}(t), \\
i\dot{C}_{10}(t) &= \Delta_3 C_{10}(t) + J C_{01}(t) + \xi C_{00}(t), \\
i\dot{C}_{02}(t) &= 2\Delta_6 C_{02}(t) + \sqrt{2} J C_{11}(t), \\
i\dot{C}_{11}(t) &= (\Delta_5 + \Delta_6) C_{11}(t) + \sqrt{2} J C_{20}(t) + \sqrt{2} J C_{02}(t) \\
&\quad + \xi C_{01}(t), \\
i\dot{C}_{20}(t) &= 2\Delta_5 C_{20}(t) + \sqrt{2} J C_{11}(t) + \sqrt{2} \xi C_{10}(t), \\
i\dot{C}_{03}(t) &= 3\Delta_8 C_{03}(t) + \sqrt{3} J C_{12}(t), \\
i\dot{C}_{12}(t) &= (\Delta_7 + 2\Delta_8) C_{12}(t) + 2 J C_{21}(t) + \sqrt{3} J C_{03}(t) \\
&\quad + \xi C_{02}(t), \\
i\dot{C}_{21}(t) &= (2\Delta_7 + \Delta_8) C_{21}(t) + \sqrt{3} J C_{30}(t) + 2 J C_{12}(t) \\
&\quad + \sqrt{2} \xi C_{11}(t), \\
i\dot{C}_{30}(t) &= 3\Delta_7 C_{30}(t) + \sqrt{3} J C_{21}(t) + \sqrt{3} \xi C_{20}(t), \quad (27)
\end{aligned}$$

where

$$\begin{aligned}
\Delta_3 &= \Delta_1 - i\gamma/2, & \Delta_4 &= \Delta_2 - i\gamma/2, \\
\Delta_5 &= \Delta_3 + \chi, & \Delta_6 &= \Delta_4 + \chi, \\
\Delta_7 &= \Delta_5 + \chi, & \Delta_8 &= \Delta_6 + \chi. \quad (28)
\end{aligned}$$

By considering the initial condition $C_{00}(0) = 1$ and setting $\dot{C}_{mn}(0) = 0$, we can obtain the steady-state solutions of the probability amplitudes

$$\begin{aligned}
C_{10} &= \frac{\xi \Delta_4}{\eta_1}, & C_{01} &= \frac{-\xi J}{\eta_1}, \\
C_{02} &= \frac{J^2 \xi^2 \sigma_1}{\sqrt{2} \eta_1 \eta_2 \sigma_2}, & C_{11} &= -\frac{J \xi^2 \Delta_6 \sigma_1}{\eta_1 \eta_2}, \\
C_{20} &= \frac{\xi^2 (\Delta_4 \Delta_6 / \sigma_1 + J^2 \chi)}{\sqrt{2} \eta_1 \eta_2 \sigma_2}, \\
C_{03} &= -\frac{J^3 \xi^3 \Gamma_4}{\sqrt{6} \sigma_2 \mu \eta_1 \eta_2}, & C_{12} &= \frac{J^2 \xi^3 \Delta_8 \Gamma_4}{\sqrt{2} \sigma_2 \mu \eta_1 \eta_2}, \\
C_{21} &= \frac{J \xi^3 [\Gamma_3 - \Delta_3 \eta_3 (\Delta_3 + 4\chi)]}{\sqrt{2} \sigma_2 \mu \eta_1 \eta_2}, \\
C_{30} &= \frac{\xi^3 (\eta_3 \Gamma_1 - \Delta_8 \Gamma_2)}{\sqrt{6} \sigma_2 \mu \eta_1 \eta_2}, \quad (29)
\end{aligned}$$

with

$$\begin{aligned}
\sigma_1 &= \Delta_4 + \Delta_5, & \sigma_2 &= \Delta_5 + \Delta_6, \\
\sigma_3 &= \Delta_7 + \Delta_8, & \zeta &= \sigma_2^2 + \sigma_3 \Delta_7 - 4 J^2,
\end{aligned}$$

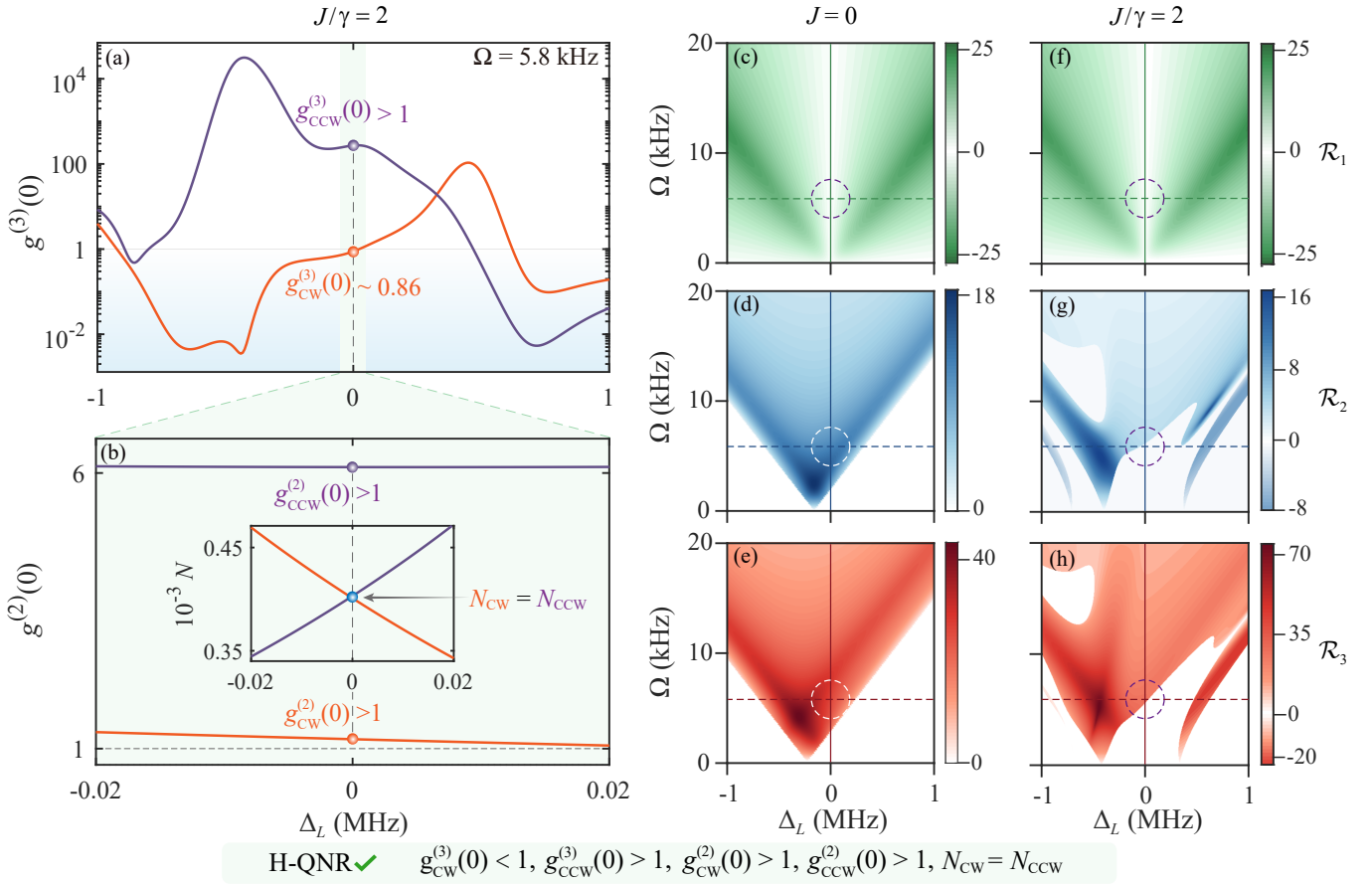


FIG. 3. The backscattering-induced higher-order quantum nonreciprocity. (a, b) The correlation functions $g^{(3)}(0)$, $g^{(2)}(0)$ and the mean photon number N versus the optical detuning Δ_L for $J/\gamma = 2$ and $\Omega = 5.8$ kHz. (c)-(h) For the generation of higher-order quantum nonreciprocity, the comparison between the cases with and without backscattering. The other parameters are the same as those in Fig. 1.

$$\begin{aligned} \eta_1 &= J^2 - \Delta_3 \Delta_4, & \eta_2 &= J^2 - \Delta_5 \Delta_6, \\ \eta_3 &= J^2 - \Delta_7 \Delta_8, & \mu &= \eta_3 (\eta_3 - 2\sigma_3^2), \\ \Gamma_1 &= (\sigma_3 + \Delta_7) (J^2 \chi + \sigma_2 \Delta_4 \Delta_6), \\ \Gamma_2 &= J^2 [2\sigma_1 (J^2 + 2\sigma_3 \Delta_6) - \chi \zeta] + \sigma_2 \Delta_4 \Delta_6 \zeta, \\ \Gamma_3 &= (2\Delta_8^2 - \eta_3) [J^2 \chi + \Delta_6 (\sigma_2 \Delta_4 + 2\sigma_1 \Delta_7)], \\ \Gamma_4 &= \sigma_1 (\eta_3 - 4\Delta_6 \Delta_7) - 2 (J^2 \chi + \sigma_2 \Delta_4 \Delta_6). \end{aligned} \quad (30)$$

The probabilities of finding m photons in the CW and n photons in the CCW modes are given by

$$P_{mn} = \frac{|C_{mn}|^2}{\mathcal{M}}, \quad (31)$$

with the normalization coefficient

$$\mathcal{M} = \sum_{N=0}^3 \sum_{m=0}^N |C_{mn}|^2. \quad (32)$$

The mean photon number is expressed

$$N = \langle \hat{a}_1^\dagger \hat{a}_1 \rangle \simeq \frac{\Delta_4^2 \xi^2}{\eta_1^2}. \quad (33)$$

The second-order correlation function is written as

$$g^{(2)}(0) = \frac{\langle \hat{a}_1^{\dagger 2} \hat{a}_1^2 \rangle}{\langle \hat{a}_1^\dagger \hat{a}_1 \rangle^2} \simeq \frac{\eta_1^2 (\Delta_4 \Delta_6 / \sigma_2 + J^2 \chi)^2}{\eta_2^2 \sigma_2^2 \Delta_4^4}. \quad (34)$$

The correlation function can be calculated numerically by solving the quantum master equation [90, 91]

$$\dot{\rho} = i[\hat{\rho}, \hat{H}_2] + \sum_{j=1,2} \frac{\gamma}{2} (2\hat{a}_j \hat{\rho} \hat{a}_j^\dagger - \hat{a}_j^\dagger \hat{a}_j \hat{\rho} - \hat{\rho} \hat{a}_j^\dagger \hat{a}_j). \quad (35)$$

The photon-number probability is $P_{mn} = \langle m, n | \hat{\rho}_{\text{ss}} | m, n \rangle$, which can be obtained from the steady-state solutions $\hat{\rho}_{\text{ss}}$ of the master equation.

Figure 2 shows quantum and classical nonreciprocities with backscattering. In Fig. 2(b), we find that the switch between CNR and QNR can still be achieved by tuning the angular velocity Ω after considering the effect of backscattering. When Ω from 0 to 6 kHz, the classical nonreciprocity ($\mathcal{R}_1 \neq 0$) appears, but there is no quantum nonreciprocity ($\mathcal{R}_2 = 0$). Adding Ω beyond 17 kHz, the opposite occurs.

As shown in Fig. 2(c), for $J/\gamma = 2$, the number of peaks of N increased from one to two, compared

with an ideal resonator [Fig. 1]. A similar feature can also be identified in the number of dips of $g^{(2)}(0)$ in Fig. 2(d). The reason is that the energy level splitting caused by backscattering provides the possibility of more photon jumps. This means we can explore the richer significance of nonreciprocity by combining backscattering and mechanical rotation.

Further, we extend our research to the higher-order quantum nonreciprocity of this system. The third-order correlation function can be obtained analytically as

$$g^{(3)}(0) = \frac{\langle \hat{a}_1^{\dagger 3} \hat{a}_1^3 \rangle}{\langle \hat{a}_1^{\dagger} \hat{a}_1 \rangle^3} \simeq \frac{\eta_1^4 (\eta_3 \Gamma_1 - \Delta_8 \Gamma_2)^2}{\mu^2 \eta_2^2 \sigma_2^2 \Delta_4^6}. \quad (36)$$

Similar to Eq. (7), we define a higher-order quantum nonreciprocity ratio \mathcal{R}_3 , which are written as

$$\mathcal{R}_3 = 10 \log_{10} \frac{g_{\text{CCW}}^{(3)}(0)}{g_{\text{CW}}^{(3)}(0)}. \quad (37)$$

We set $\mathcal{R}_3 = 0$ for the cases of both $g_{\text{CCW}}^{(3)}(0)$ and $g_{\text{CW}}^{(3)}(0)$ are smaller or larger than 1. The difference is that the condition of higher-order quantum nonreciprocity (H-QNR) not only needs to satisfy $\mathcal{R}_3 \neq 0$, but also needs to satisfy the condition of reciprocity of classical mean photon number ($\mathcal{R}_1 = 0$) and quantum second-order correlation function ($\mathcal{R}_2 = 0$).

Figures 3(a) and 3(b) show that higher-order quantum nonreciprocity occurs around $\Delta_L = 0$. At this point, for different input directions, the third-order correlation functions are nonreciprocal ($g_{\text{CW}}^{(3)}(0) \sim 0.86$, $g_{\text{CCW}}^{(3)}(0) \sim 272.68$), but the second-order correlation functions and the mean photon numbers are reciprocal, i.e., $g_{\text{CW}}^{(2)}(0) > 1$, $g_{\text{CCW}}^{(2)}(0) > 1$, and $N_{\text{CW}} = N_{\text{CCW}}$. As far as we know, this pure higher-order quantum nonreciprocity has not been revealed in previous works on the nonreciprocal effect.

To clearly show the difference in nonreciprocities between the ideal cavity ($J = 0$) and the realistic cavity ($J/\gamma = 2$), we compare the nonreciprocity ratios of the above different cases, as shown in Figs. 3(c-h). We find that backscattering has a small effect on the classical nonreciprocity [see Figs. 3(c) and 3(f)], but a large effect

on the quantum nonreciprocity, e.g., the negative value of \mathcal{R}_3 appears in Fig. 3(h). By comparison, we note that the higher-order quantum nonreciprocity occurs in the realistic cavity, due to the effect of backscattering, but not in an ideal cavity.

V. CONCLUSIONS

In summary, we study the coherent switch of classical and quantum nonreciprocities of photons, and realize the higher-order quantum nonreciprocity by using a spinning Kerr resonator. Our findings contain three main features. First, we show a single device switching between a classical isolator and a purely quantum directional system by adjusting multiple degrees of freedom (the optical detuning Δ_L and angular velocity Ω). Furthermore, we present the higher-order quantum nonreciprocity for the first time, which provides a richer degree of freedom for one-way optical control, i.e., it is available to achieve one-way quantum communication while classical communication is reciprocal. More interestingly, in practical devices, the backscattering is unavoidable, but it can induce higher-order quantum nonreciprocity. These results offer the possibility of new developments in nonreciprocal devices, as well as have potential applications in nanoparticle sensing. We believe that our work can be extended to spinning photonics and spinning optomechanics with similar backscattering.

VI. ACKNOWLEDGMENTS

H.J. is supported by the National Natural Science Foundation of China (Grants No.11935006, No.11774086, and No.1217050862) and the Science and Technology Innovation Program of Hunan Province (Grant No.2020RC4047). R.H. is supported by the Japan Society for the Promotion of Science (JSPS) Post-doctoral Fellowships for Research in Japan (No. P22018).

[1] Y. Shoji and T. Mizumoto, Magneto-optical nonreciprocal devices in silicon photonics, *Sci. Technol. Adv. Mater.* **15**, 014602 (2014).

[2] J. Adam, L. Davis, G. Dionne, E. Schloemann, and S. Stitzer, Ferrite devices and materials, *IEEE Trans. Microw. Theory Tech.* **50**, 721 (2002).

[3] H. Dötsch, N. Bahlmann, O. Zhirovskyy, M. Hammer, L. Wilkens, R. Gerhardt, P. Hertel, and A. F. Popkov, Applications of magneto-optical waveguides in integrated optics: Review, *J. Opt. Soc. Am. B, JOSAB* **22**, 240 (2005).

[4] Z. Yu and S. Fan, Complete optical isolation created by indirect interband photonic transitions, *Nature Photon* **3**, 91 (2009).

[5] M. S. Kang, A. Butsch, and P. S. J. Russell, Reconfigurable light-driven opto-acoustic isolators in photonic crystal fibre, *Nature Photon* **5**, 549 (2011).

[6] N. A. Estep, D. L. Sounas, J. Soric, and A. Alù, Magnetic-free non-reciprocity and isolation based on parametrically modulated coupled-resonator loops, *Nature Phys* **10**, 923 (2014).

[7] L. D. Tzuang, K. Fang, P. Nussenzveig, S. Fan, and M. Lipson, Non-reciprocal phase shift induced by an effective magnetic flux for light, *Nature Photon* **8**, 701 (2014).

[8] T. T. Koutserimpas and R. Fleury, Nonreciprocal gain in non-hermitian time-floquet systems, *Phys. Rev. Lett.* **120**, 087401 (2018).

[9] E. A. Kittlaus, N. T. Otterstrom, P. Kharel, S. Gertler, and P. T. Rakich, Non-reciprocal interband brillouin modulation, *Nature Photon* **12**, 613 (2018).

[10] X. Guo, Y. Ding, Y. Duan, and X. Ni, Nonreciprocal metasurface with space-time phase modulation, *Light Sci Appl* **8**, 123 (2019).

[11] X. Wang, G. Ptitsyn, V. S. Asadchy, A. Díaz-Rubio, M. S. Mirmoosa, S. Fan, and S. A. Tretyakov, Nonreciprocity in bianisotropic systems with uniform time modulation, *Phys. Rev. Lett.* **125**, 266102 (2020).

[12] L. Fan, J. Wang, L. T. Varghese, H. Shen, B. Niu, Y. Xuan, A. M. Weiner, and M. Qi, An all-silicon passive optical diode, *Science* **335**, 447 (2012).

[13] H. Z. Shen, Y. H. Zhou, and X. X. Yi, Quantum optical diode with semiconductor microcavities, *Phys. Rev. A* **90**, 023849 (2014).

[14] Q.-T. Cao, H. Wang, C.-H. Dong, H. Jing, R.-S. Liu, X. Chen, L. Ge, Q. Gong, and Y.-F. Xiao, Experimental demonstration of spontaneous chirality in a nonlinear microresonator, *Phys. Rev. Lett.* **118**, 033901 (2017).

[15] X.-W. Xu, Y. Li, B. Li, H. Jing, and A.-X. Chen, Nonreciprocity via nonlinearity and synthetic magnetism, *Phys. Rev. Applied* **13**, 044070 (2020).

[16] Q.-T. Cao, R. Liu, H. Wang, Y.-K. Lu, C.-W. Qiu, S. Rotter, Q. Gong, and Y.-F. Xiao, Reconfigurable symmetry-broken laser in a symmetric microcavity, *Nat Commun* **11**, 1136 (2020).

[17] S. Manipatruni, J. T. Robinson, and M. Lipson, Optical nonreciprocity in optomechanical structures, *Phys. Rev. Lett.* **102**, 213903 (2009).

[18] C.-H. Dong, Z. Shen, C.-L. Zou, Y.-L. Zhang, W. Fu, and G.-C. Guo, Brillouin-scattering-induced transparency and non-reciprocal light storage, *Nat Commun* **6**, 6193 (2015).

[19] J. Kim, M. C. Kuzyk, K. Han, H. Wang, and G. Bahl, Non-reciprocal brillouin scattering induced transparency, *Nature Phys* **11**, 275 (2015).

[20] Z. Shen, Y.-L. Zhang, Y. Chen, C.-L. Zou, Y.-F. Xiao, X.-B. Zou, F.-W. Sun, G.-C. Guo, and C.-H. Dong, Experimental realization of optomechanically induced non-reciprocity, *Nature Photon* **10**, 657 (2016).

[21] F. Ruesink, M.-A. Miri, A. Alù, and E. Verhagen, Nonreciprocity and magnetic-free isolation based on optomechanical interactions, *Nat Commun* **7**, 13662 (2016).

[22] S. Hua, J. Wen, X. Jiang, Q. Hua, L. Jiang, and M. Xiao, Demonstration of a chip-based optical isolator with parametric amplification, *Nat Commun* **7**, 13657 (2016).

[23] N. R. Bernier, L. D. Tóth, A. Koottandavida, M. A. Ioannou, D. Malz, A. Nunnenkamp, A. K. Feofanov, and T. J. Kippenberg, Nonreciprocal reconfigurable microwave optomechanical circuit, *Nat Commun* **8**, 604 (2017).

[24] M.-A. Miri, F. Ruesink, E. Verhagen, and A. Alù, Optical nonreciprocity based on optomechanical coupling, *Phys. Rev. Appl.* **7**, 064014 (2017).

[25] Z. Shen, Y.-L. Zhang, Y. Chen, F.-W. Sun, X.-B. Zou, G.-C. Guo, C.-L. Zou, and C.-H. Dong, Reconfigurable optomechanical circulator and directional amplifier, *Nat Commun* **9**, 1797 (2018).

[26] A. Rosario Hamann, C. Müller, M. Jerger, M. Zanner, J. Combes, M. Pletyukhov, M. Weides, T. M. Stace, and A. Fedorov, Nonreciprocity realized with quantum nonlinearity, *Phys. Rev. Lett.* **121**, 123601 (2018).

[27] D. L. Sounas and A. Alù, Nonreciprocity based on nonlinear resonances, *IEEE Antennas Wirel. Propag. Lett.* **17**, 1958 (2018).

[28] L. Mercier de Lépinay, E. Damskägg, C. F. Ockeloen-Korppi, and M. A. Sillanpää, Realization of directional amplification in a microwave optomechanical device, *Phys. Rev. Applied* **11**, 034027 (2019).

[29] X. Xu, Y. Zhao, H. Wang, H. Jing, and A. Chen, Quantum nonreciprocity in quadratic optomechanics, *Photon. Res., PRJ* **8**, 143 (2020).

[30] L. Tang, J. Tang, H. Wu, J. Zhang, M. Xiao, and K. Xia, Broad-intensity-range optical nonreciprocity based on feedback-induced kerr nonlinearity, *Photon. Res., PRJ* **9**, 1218 (2021).

[31] Z. Shen, Y.-L. Zhang, Y. Chen, Y.-F. Xiao, C.-L. Zou, G.-C. Guo, and C.-H. Dong, Nonreciprocal frequency conversion and mode routing in a microresonator, *Phys. Rev. Lett.* **130**, 013601 (2023).

[32] H. Ramezani, T. Kottos, R. El-Ganainy, and D. N. Christodoulides, Unidirectional nonlinear PT-symmetric optical structures, *Phys. Rev. A* **82**, 043803 (2010).

[33] B. Peng, S. K. Özdemir, F. Lei, F. Monifi, M. Gianfreda, G. L. Long, S. Fan, F. Nori, C. M. Bender, and L. Yang, Parity-time-symmetric whispering-gallery microcavities, *Nature Phys* **10**, 394 (2014).

[34] L. Chang, X. Jiang, S. Hua, C. Yang, J. Wen, L. Jiang, G. Li, G. Wang, and M. Xiao, Parity-time symmetry and variable optical isolation in active-passive-coupled microresonators, *Nature Photon* **8**, 524 (2014).

[35] X. Huang, C. Lu, C. Liang, H. Tao, and Y.-C. Liu, Loss-induced nonreciprocity, *Light Sci Appl* **10**, 30 (2021).

[36] L. Tang, J. Tang, M. Chen, F. Nori, M. Xiao, and K. Xia, Quantum squeezing induced optical nonreciprocity, *Phys. Rev. Lett.* **128**, 083604 (2022).

[37] D.-W. Wang, H.-T. Zhou, M.-J. Guo, J.-X. Zhang, J. Evers, and S.-Y. Zhu, Optical diode made from a moving photonic crystal, *Phys. Rev. Lett.* **110**, 093901 (2013).

[38] K. Xia, F. Nori, and M. Xiao, Cavity-free optical isolators and circulators using a chiral cross-kerr nonlinearity, *Phys. Rev. Lett.* **121**, 203602 (2018).

[39] S. Zhang, Y. Hu, G. Lin, Y. Niu, K. Xia, J. Gong, and S. Gong, Thermal-motion-induced non-reciprocal quantum optical system, *Nature Photon* **12**, 744 (2018).

[40] C. Liang, B. Liu, A.-N. Xu, X. Wen, C. Lu, K. Xia, M. K. Tey, Y.-C. Liu, and L. You, Collision-induced broadband optical nonreciprocity, *Phys. Rev. Lett.* **125**, 123901 (2020).

[41] M.-X. Dong, K.-Y. Xia, W.-H. Zhang, Y.-C. Yu, Y.-H. Ye, E.-Z. Li, L. Zeng, D.-S. Ding, B.-S. Shi, G.-C. Guo, and F. Nori, All-optical reversible single-photon isolation at room temperature, *Sci. Adv.* **7**, eabe8924 (2021).

[42] F. Song, Z. Wang, E. Li, B. Yu, and Z. Huang, Nonreciprocity with structured light using optical pumping in hot atoms, *Phys. Rev. Appl.* **18**, 024027

(2022).

[43] H. Lü, Y. Jiang, Y.-Z. Wang, and H. Jing, Optomechanically induced transparency in a spinning resonator, *Photon. Res., PRJ* **5**, 367 (2017).

[44] S. Maayani, R. Dahan, Y. Kligerman, E. Moses, A. U. Hassan, H. Jing, F. Nori, D. N. Christodoulides, and T. Carmon, Flying couplers above spinning resonators generate irreversible refraction, *Nature* **558**, 569 (2018).

[45] Y. Jiang, S. Maayani, T. Carmon, F. Nori, and H. Jing, Nonreciprocal phonon laser, *Phys. Rev. Applied* **10**, 064037 (2018).

[46] R. Huang, A. Miranowicz, J.-Q. Liao, F. Nori, and H. Jing, Nonreciprocal photon blockade, *Phys. Rev. Lett.* **121**, 153601 (2018).

[47] B. Li, R. Huang, X. Xu, A. Miranowicz, and H. Jing, Nonreciprocal unconventional photon blockade in a spinning optomechanical system, *Photon. Res., PRJ* **7**, 630 (2019).

[48] K. Wang, Q. Wu, Y.-F. Yu, and Z.-M. Zhang, Nonreciprocal photon blockade in a two-mode cavity with a second-order nonlinearity, *Phys. Rev. A* **100**, 053832 (2019).

[49] H. Z. Shen, Q. Wang, J. Wang, and X. X. Yi, Nonreciprocal unconventional photon blockade in a driven dissipative cavity with parametric amplification, *Phys. Rev. A* **101**, 013826 (2020).

[50] Y.-W. Jing, H.-Q. Shi, and X.-W. Xu, Nonreciprocal photon blockade and directional amplification in a spinning resonator coupled to a two-level atom, *Phys. Rev. A* **104**, 033707 (2021).

[51] Y.-F. Jiao, S.-D. Zhang, Y.-L. Zhang, A. Miranowicz, L.-M. Kuang, and H. Jing, Nonreciprocal optomechanical entanglement against backscattering losses, *Phys. Rev. Lett.* **125**, 143605 (2020).

[52] Z.-B. Yang, J.-S. Liu, A.-D. Zhu, H.-Y. Liu, and R.-C. Yang, Nonreciprocal transmission and nonreciprocal entanglement in a spinning microwave magnomechanical system, *Ann. Phys.* **532**, 2000196 (2020).

[53] Y.-l. Ren, Nonreciprocal optical-microwave entanglement in a spinning magnetic resonator, *Opt. Lett., OL* **47**, 1125 (2022).

[54] Y.-F. Jiao, J.-X. Liu, Y. Li, R. Yang, L.-M. Kuang, and H. Jing, Nonreciprocal enhancement of remote entanglement between nonidentical mechanical oscillators, *Phys. Rev. Appl.* **18**, 064008 (2022).

[55] I. M. Mirza, W. Ge, and H. Jing, Optical nonreciprocity and slow light in coupled spinning optomechanical resonators, *Opt. Express, OE* **27**, 25515 (2019).

[56] W.-A. Li, G.-Y. Huang, J.-P. Chen, and Y. Chen, Nonreciprocal enhancement of optomechanical second-order sidebands in a spinning resonator, *Phys. Rev. A* **102**, 033526 (2020).

[57] D.-W. Zhang, L.-L. Zheng, C. You, C.-S. Hu, Y. Wu, and X.-Y. Lü, Nonreciprocal chaos in a spinning optomechanical resonator, *Phys. Rev. A* **104**, 033522 (2021).

[58] B. Li, S. K. Özdemir, X.-W. Xu, L. Zhang, L.-M. Kuang, and H. Jing, Nonreciprocal optical solitons in a spinning kerr resonator, *Phys. Rev. A* **103**, 053522 (2021).

[59] Y. Xu, J.-Y. Liu, W. Liu, and Y.-F. Xiao, Nonreciprocal phonon laser in a spinning microwave magnomechanical system, *Phys. Rev. A* **103**, 053501 (2021).

[60] X. Shang, H. Xie, G. Lin, and X. Lin, Nonreciprocity steered with a spinning resonator, *Photonics* **9**, 585 (2022).

[61] Z. Yang, Y. Cheng, N. Wang, Y. Chen, and S. Wang, Nonreciprocal light propagation induced by a subwavelength spinning cylinder, *Opt. Express, OE* **30**, 27993 (2022).

[62] R. Fleury, D. L. Sounas, C. F. Sieck, M. R. Haberman, and A. Alù, Sound isolation and giant linear nonreciprocity in a compact acoustic circulator, *Science* **343**, 516 (2014).

[63] A. B. Khanikaev, R. Fleury, S. H. Mousavi, and A. Alù, Topologically robust sound propagation in an angular-momentum-biased graphene-like resonator lattice, *Nat Commun* **6**, 1 (2015).

[64] X. Xu, Q. Wu, H. Chen, H. Nassar, Y. Chen, A. Norris, M. R. Haberman, and G. Huang, Physical observation of a robust acoustic pumping in waveguides with dynamic boundary, *Phys. Rev. Lett.* **125**, 253901 (2020).

[65] H. Jing, H. Lü, S. K. Özdemir, T. Carmon, and F. Nori, Nanoparticle sensing with a spinning resonator, *Optica, OPTICA* **5**, 1424 (2018).

[66] J. Ahn, Z. Xu, J. Bang, P. Ju, X. Gao, and T. Li, Ultrasensitive torque detection with an optically levitated nanorotor, *Nat. Nanotechnol.* **15**, 89 (2020).

[67] H. Zhang, R. Huang, S.-D. Zhang, Y. Li, C.-W. Qiu, F. Nori, and H. Jing, Breaking anti-pt symmetry by spinning a resonator, *Nano Lett.* **20**, 7594 (2020).

[68] X. Mao, H. Yang, D. Long, M. Wang, P.-Y. Wen, Y.-Q. Hu, B.-Y. Wang, G.-Q. Li, J.-C. Gao, and G.-L. Long, Experimental demonstration of mode-matching and sagnac effect in a millimeter-scale wedged resonator gyroscope, *Photon. Res., PRJ* **10**, 2115 (2022).

[69] I. H. Grinberg, M. Lin, C. Harris, W. A. Benalcazar, C. W. Peterson, T. L. Hughes, and G. Bahl, Robust temporal pumping in a magneto-mechanical topological insulator, *Nat Commun* **11**, 1 (2020).

[70] G. Xu, K. Dong, Y. Li, H. Li, K. Liu, L. Li, J. Wu, and C.-W. Qiu, Tunable analog thermal material, *Nat Commun* **11**, 6028 (2020).

[71] L. Dong and Y. V. Kartashov, Rotating multidimensional quantum droplets, *Phys. Rev. Lett.* **126**, 244101 (2021).

[72] Z. Zhu, X. Ren, W. Sha, M. Xiao, R. Hu, and X. Luo, Inverse design of rotating metadevice for adaptive thermal cloaking, *International Journal of Heat and Mass Transfer* **176**, 121417 (2021).

[73] L. Xu, J. Liu, P. Jin, G. Xu, J. Li, X. Ouyang, Y. Li, C.-W. Qiu, and J. Huang, Blackhole-inspired thermal trapping with graded heat-conduction metadevices, *National Science Review* , nwac159 (2022).

[74] P. Yang, M. Li, X. Han, H. He, G. Li, C.-L. Zou, P. Zhang, and T. Zhang, Non-reciprocal cavity polariton, *arXiv:1911.10300* .

[75] A. Graf, S. D. Rogers, J. Staffa, U. A. Javid, D. H. Griffith, and Q. Lin, Nonreciprocity in photon pair correlations of classically reciprocal systems, *Phys. Rev. Lett.* **128**, 213605 (2022).

[76] C. Gonzalez-Ballester, A. Gonzalez-Tudela, F. J. Garcia-Vidal, and E. Moreno, Chiral route to spontaneous entanglement generation, *Phys. Rev. B* **92**, 155304 (2015).

[77] H. J. Kimble, The quantum internet, *Nature* **453**, 1023 (2008).

[78] P. Lodahl, S. Mahmoodian, S. Stobbe, A. Rauschenbeutel, P. Schneeweiss, J. Volz, H. Pichler, and P. Zoller, Chiral quantum optics, *Nature* **541**, 473 (2017).

[79] S. A. H. Gangaraj, G. W. Hanson, and M. Antezza, Robust entanglement with three-dimensional nonreciprocal photonic topological insulators, *Phys. Rev. A* **95**, 063807 (2017).

[80] R. Fleury, D. Sounas, and A. Alù, An invisible acoustic sensor based on parity-time symmetry, *Nat Commun* **6**, 5905 (2015).

[81] T. Yang, X. Bai, D. Gao, L. Wu, B. Li, J. T. L. Thong, and C.-W. Qiu, Invisible sensors: Simultaneous sensing and camouflaging in multiphysical fields, *Adv. Mater.* **27**, 7752 (2015).

[82] G. B. Malykin, The sagnac effect: Correct and incorrect explanations, *Phys.-Usp.* **43**, 1229 (2000).

[83] J. A. Zielińska and M. W. Mitchell, “Self-tuning optical resonator,” *Opt. Lett.* **42**, 5298 (2017).

[84] K. J. Vahala, “Optical microcavities,” *Nature (London)* **424**, 839 (2003).

[85] S. M. Spillane, T. J. Kippenberg, K. J. Vahala, K. W. Goh, E. Wilcut, and H. J. Kimble, “Ultrahigh- Q toroidal microresonators for cavity quantum electrodynamics,” *Phys. Rev. A* **71**, 013817 (2005).

[86] N. G. Pavlov, G. Lihachev, S. Koptyaev, E. Lucas, M. Karpov, N. M. Kondratiev, I. A. Bilenko, T. J. Kippenberg, and M. L. Gorodetsky, “Soliton dual frequency combs in crystalline microresonators,” *Opt. Lett.* **42**, 514 (2017).

[87] V. Huet, A. Rasoloniaina, P. Guillemé, P. Rochard, P. Féron, M. Mortier, A. Levenson, K. Bencheikh, A. Yacomotti, and Y. Dumeige, “Millisecond Photon Lifetime in a Slow-Light Microcavity,” *Phys. Rev. Lett.* **116**, 133902 (2016).

[88] M. B. Plenio and P. L. Knight, The quantum-jump approach to dissipative dynamics in quantum optics, *Rev. Mod. Phys.* **70**, 101 (1998).

[89] H. J. Carmichael, R. J. Brecha, and P. R. Rice, Quantum interference and collapse of the wavefunction in cavity qed, *Optics Communications* **82**, 73 (1991).

[90] J. R. Johansson, P. D. Nation, and F. Nori, Qutip: An open-source python framework for the dynamics of open quantum systems, *Computer Physics Communications* **183**, 1760 (2012).

[91] J. R. Johansson, P. D. Nation, and F. Nori, Qutip 2: A python framework for the dynamics of open quantum systems, *Computer Physics Communications* **184**, 1234 (2013).

[92] Z. R. Gong, H. Ian, Y.-x. Liu, C. P. Sun, and F. Nori, Effective hamiltonian approach to the kerr nonlinearity in an optomechanical system, *Phys. Rev. A* **80**, 065801 (2009).